

"ENVI Processing of AVIRIS Hyperspectral Data for Mineralogical Classification
and Morphological Delineation of El Pico de Orizaba Volcano, Mexico."

Tobin Martin

ES6973

09 May 2005

Introduction

El Pico de Orizaba (Citlaltépetl) is a Tertiary-aged stratovolcano located on the border between the Mexican states of Puebla and Veracruz, approximately 150 miles east of Mexico City. It is the third highest peak in North America at 5610 meters (18,401 feet) above sea level and is capped by the receding Jamapa glacier. El Pico is situated at the eastern edge of the Trans-Mexican Volcanic Belt (Figure 1). The volcano is of

intermediate composition with single- and multi-modal lava flows of andesite and dacite and with periodic pyroclastic events depositing ash and tuff layers.

Hydrothermal alteration minerals

are also in abundance where the exposed volcanic rock has been subjected to physical and chemical weathering processes.



Figure 1. Trans-Mexican Volcanic Belt

Purpose

This study is to investigate the utility of Airborne Visible/Infrared Imaging Spectrometer (AVIRIS) hyperspectral data manipulation to delineate morphology and mineralogy of the El Pico volcano. The resulting imagery and data will be compared to field samples collected in June 2004. Additional remotely sensed data may also be investigated, such as that from the Space Imaging, Inc. IKONOS-2 and Landsat 7 Enhanced Thematic Mapper multispectral systems.

Summary of AVIRIS Features

AVIRIS was developed by NASA at the Jet Propulsion Laboratory in Pasadena, California (Figure 2).

The AVIRIS system is composed of whiskbroom-scanned linear arrays made of silicon (visible) and indium-antimonide (infrared); it collects hyperspectral data in the range of 400 to 2500nm in 224 bands of 10nm

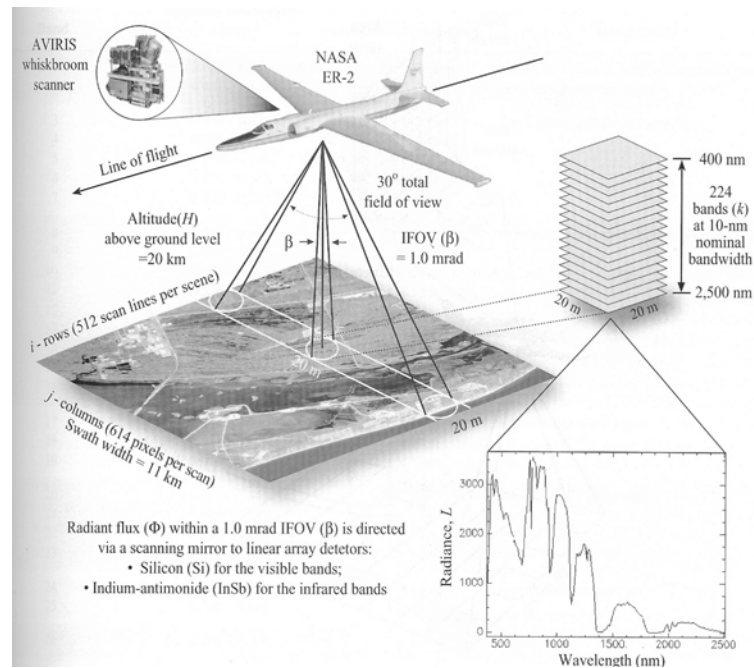


Figure 2. AVIRIS features (from Jensen, 2005).

each. AVIRIS is typically flown 20km above ground level in a NASA/ARC ER-2 aircraft; the resultant field of view is 30 degrees wide and contains 20 x 20m pixels. The radiometric resolution of AVIRIS is 16-bit—the system collects data in 12-bits and the data are processed to 16-bit integer values. AVIRIS can also be flown in low-altitude mode; however, the topography of the volcano would produce a highly variable scale of pixel resolution.

Correction Procedures

AVIRIS data provided by NASA is preprocessed to remove fundamental geometric and radiometric errors associated with the motion of the vehicle used during collection.

Several types of additional correction must be applied to remove further errors due to atmospheric effects such as absorption and scattering and geometric error related to the topography of the study area.

First, radiometric correction using FLAASH (Fast Line-of-sight Atmospheric Analysis of Spectral Hypercubes) was performed on the data. FLAASH is an extremely powerful tool for pre-processing; it removes atmospheric interference and converts radiance images to surface reflectance. Flash uses the MODTRAN4 radiation transfer code in conjunction with standard MODTRAN model atmospheres and aerosol types. A correction for the "adjacency effect"—pixel mixing due to surface-reflected radiance scattering and a function to compute the average scene visibility are also included with the utilities in FLAASH. Output images include: surface reflectance, cloud classification, and water vapor images. Spectral polishing provides artifact suppression.

The use of FLAASH requires the sensor to incorporate the following spectral ranges for atmospheric correction: 1050-1210 nm, 870-1020 nm and 770-870 nm—with a spectral resolution of 15 nm or better. The entire spectral range of the dataset must be known, as well as the Full Width Half Minimum (FWHM) for each band and any gain and offset values used to convert the (signal) digital number (DN) values to radiance, preferably available in ASCII *.txt files. The input parameters necessary for FLAASH processing are described below.

The file f941126t01p02_r03_sc07.c.img is an 11 x 9 km, calibrated AVIRIS image centered at 19.00475 N / 97.25975 W (lat/long). The data were collected at 1900 GMT on 26 November 1994. The sensor altitude was 20 km, the average ground elevation was 3.077 km (as derived from a USGS DEM), and the pixel size was 20 m. Several atmospheric models were tested, however, the FLAASH User's Guide recommended that the atmospheric model be selected according to surface air temperature. The best results were yielded from a FLAASH run using the Sub-Arctic Summer (SAS) atmospheric model. The Water Retrieval function was selected, with the water absorption feature set at 1135 nm.

The Aerosol Retrieval function was not selected due to the clear conditions; the selection of an aerosol model is unnecessary if the initial visibility is greater than 40 km. Spectral Polishing was selected using a value of 9 for the width (number of bands). AVIRIS is supported for automatic wavelength recalibration and channel definition selection; the default setting of yes to both of these is recommended by the FLAASH User's Guide.

Next, basic geometric correction was achieved by warping the FLAASH-output reflectance image to match the projection and datum of a USGS Digital Elevation Model

(DEM) of the study area. The warped reflectance image was draped over the DEM to reduce foreshortening. Due to the topographic relief in the study area, other complex geometric errors are introduced; the data will need to be meticulously re-processed before classified images can be correlated with other sources of imagery or data.

The results of the FLAASH correction include a surface reflectance image (Figure 3), a cloud classification map, and a water vapor map. However, errors during processing produced cloud classification and water vapor maps containing no data. Additional analysis and processing will be necessary to ensure proper and complete FLAASH correction.

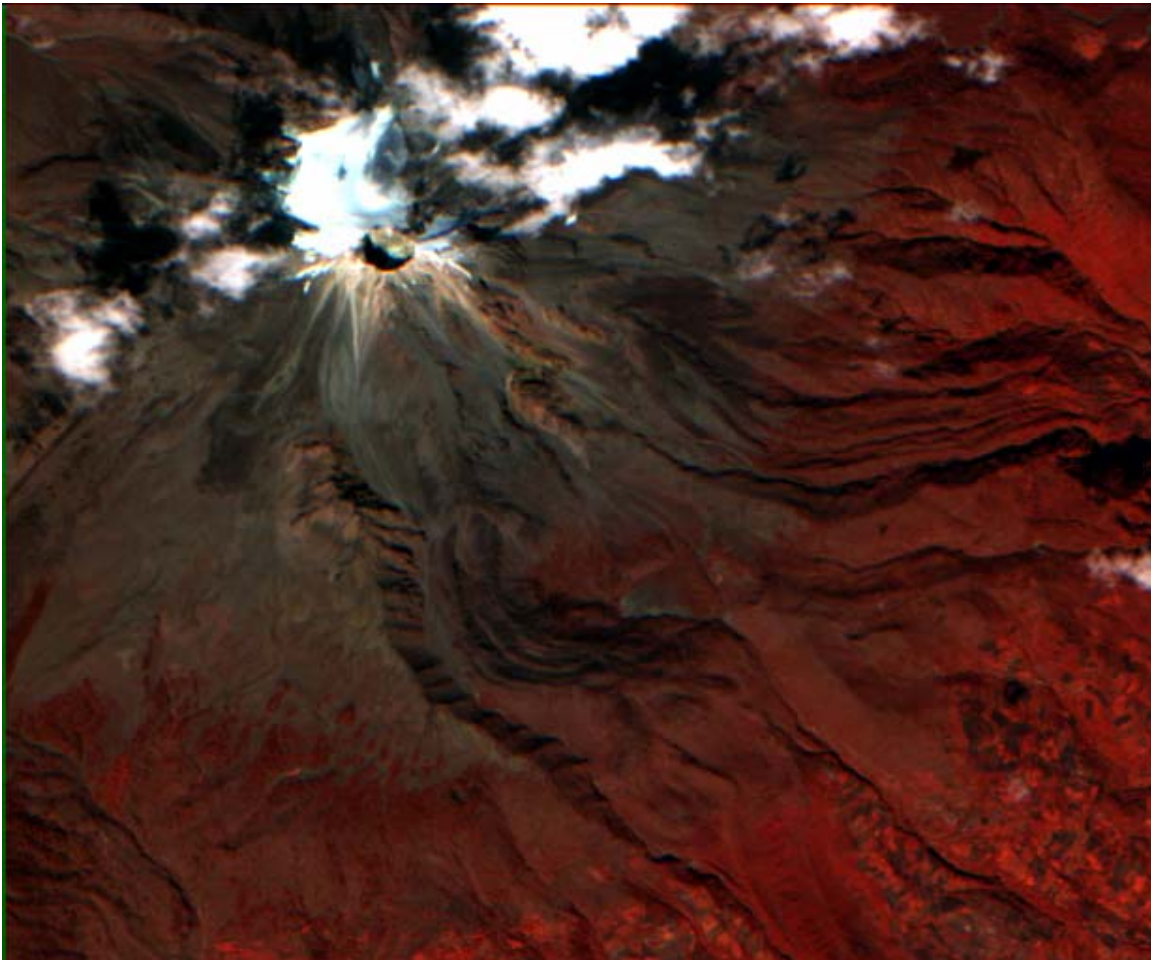


Figure 3. AVIRIS reflectance image (RGB:50,20,10) of El Pico de Orizaba.

Processing and Classification Procedures

Another useful tool in hyperspectral data analysis is to reduce the dimensionality of the data. This was accomplished by using the Minimum Noise Fraction (MNF) transformation; this applies two cascaded Principal Component Analyses (PCA's) to produce eigenimages (Figure 4) used to separate noise from useful data. A forward MNF

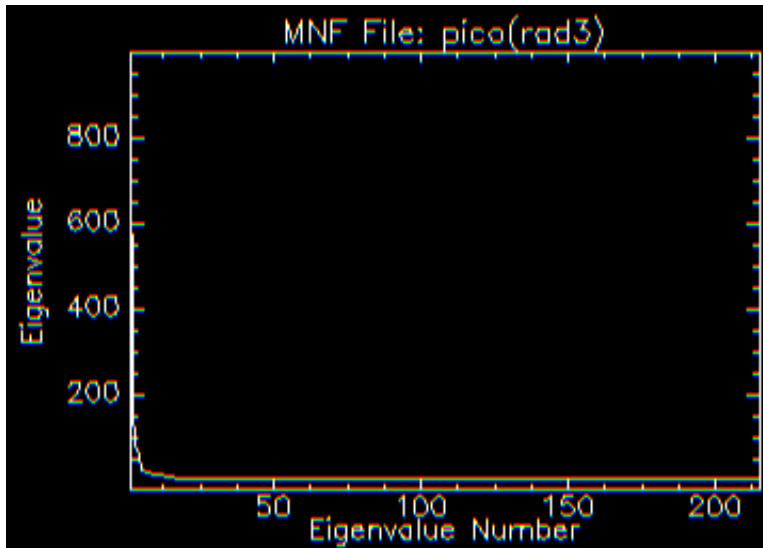


Figure 4. ENVI MNF transformation eigenvalue plot.

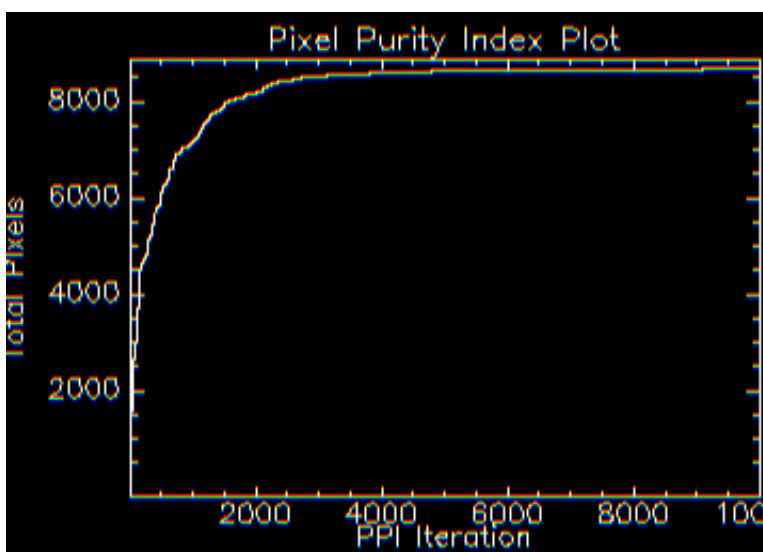


Figure 5. ENVI PPI results.

transformation was applied to the data and 41 out of 215 bands were noise-free enough for classification purposes. The resulting useful data was then processed using a Pixel Purity Index (PPI) where the threshold value was 2.5 and processed through 10000 iterations (Figure 5). The n-Dimensional Visualizer was used for endmember determination of these spectrally purest pixels. The endmembers were automatically

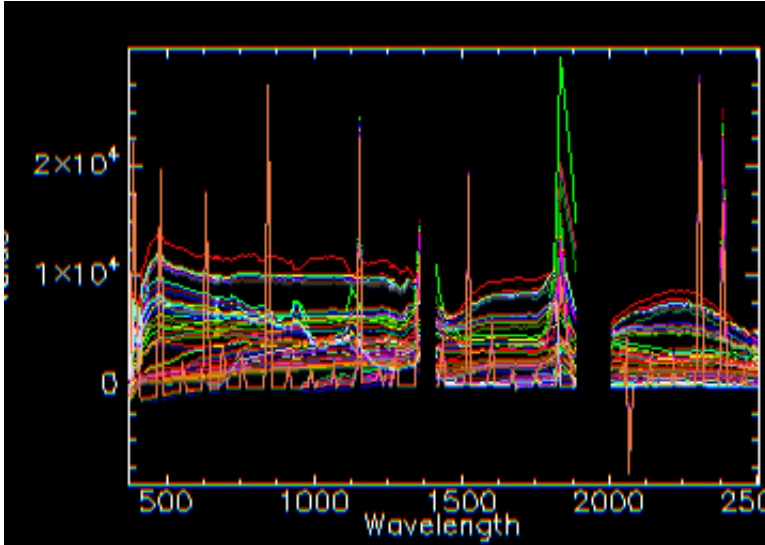


Figure 6. ENVI collected spectral endmember plot.

collected and used in the classification of the reflectance data (Figure 6). ENVI's Spectral Angle Mapper (SAM) is a powerful tool for image classification. The collected spectral endmembers were

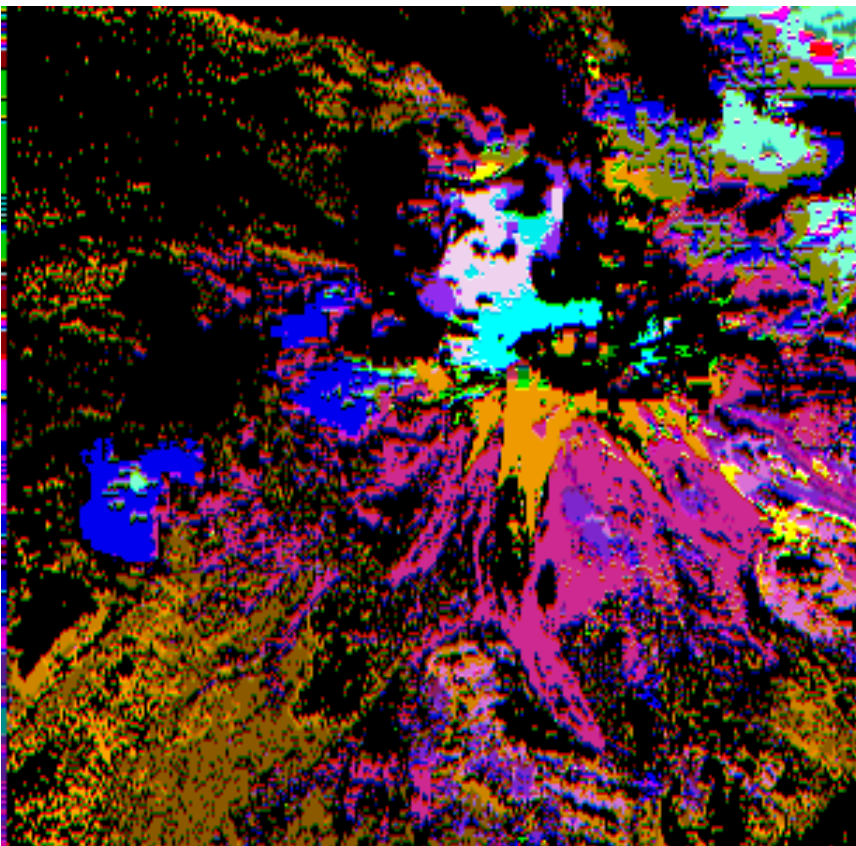


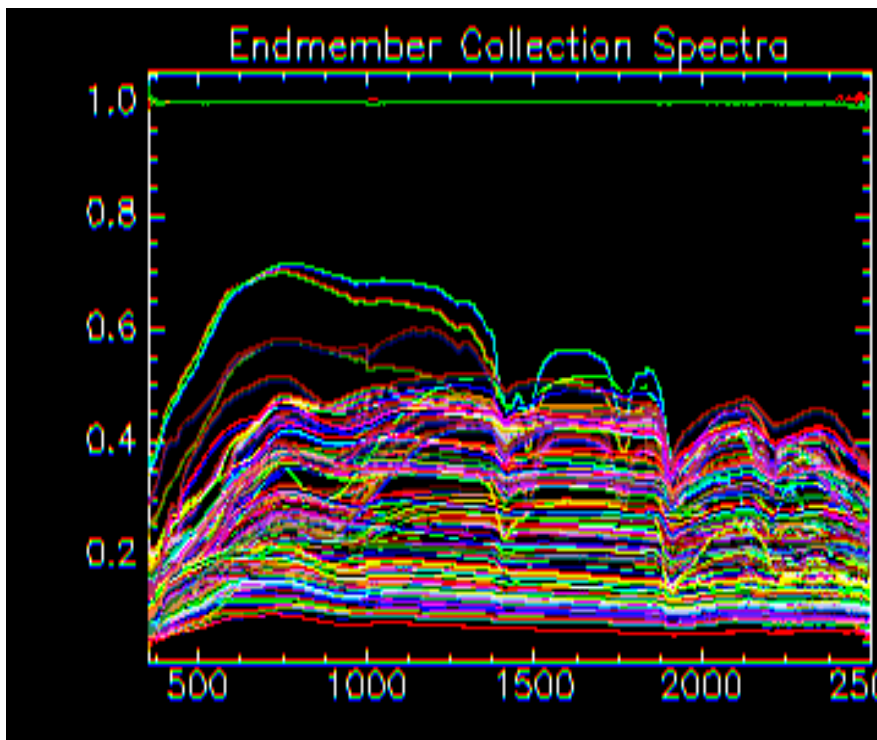
Figure 7. ENVI SAM classification using USGS reference spectra.

processed using the Spectral Analyst and matched to the USGS (Mineral) Spectral Library using Spectral Feature Fitting (SFF) and SAM matching. A subset of the SAM classification is shown in Figure 7.

Field Methods

The field samples were collected on 07 June 2004, from several locations along the eastern slope of the volcano. Near the base of the Jamapa glacier, an outcrop known locally as “El Sarcófago (The Sarcophagus),” displays signs of hydrothermal alteration and weathering; samples were collected from the base of the outcrop and from the base of the glacier.

The field samples were measured using an Applied Spectral Devices Field-Spec Pro handheld spectroradiometer. The Field-Spec Pro uses a xenon light source to measure reflectance in the range of 350 to 2500 nm; it can interpolate to 1 nm bandwidth and is calibrated using a Spectrolon (100% reflectance) white reference panel. The weathered



and fresh surfaces and any apparent coatings were measured with the spectroradiometer and the reflectance spectra were converted to a spectral library using ENVI (Figure 8).

Figure 8. Spectral library plot of field samples.

Supplemental Classification Procedures

The spectral library of field sample spectroradiometer measurements was used in conjunction with the Spectral Analyst to produce another SAM classification (Figure 9).

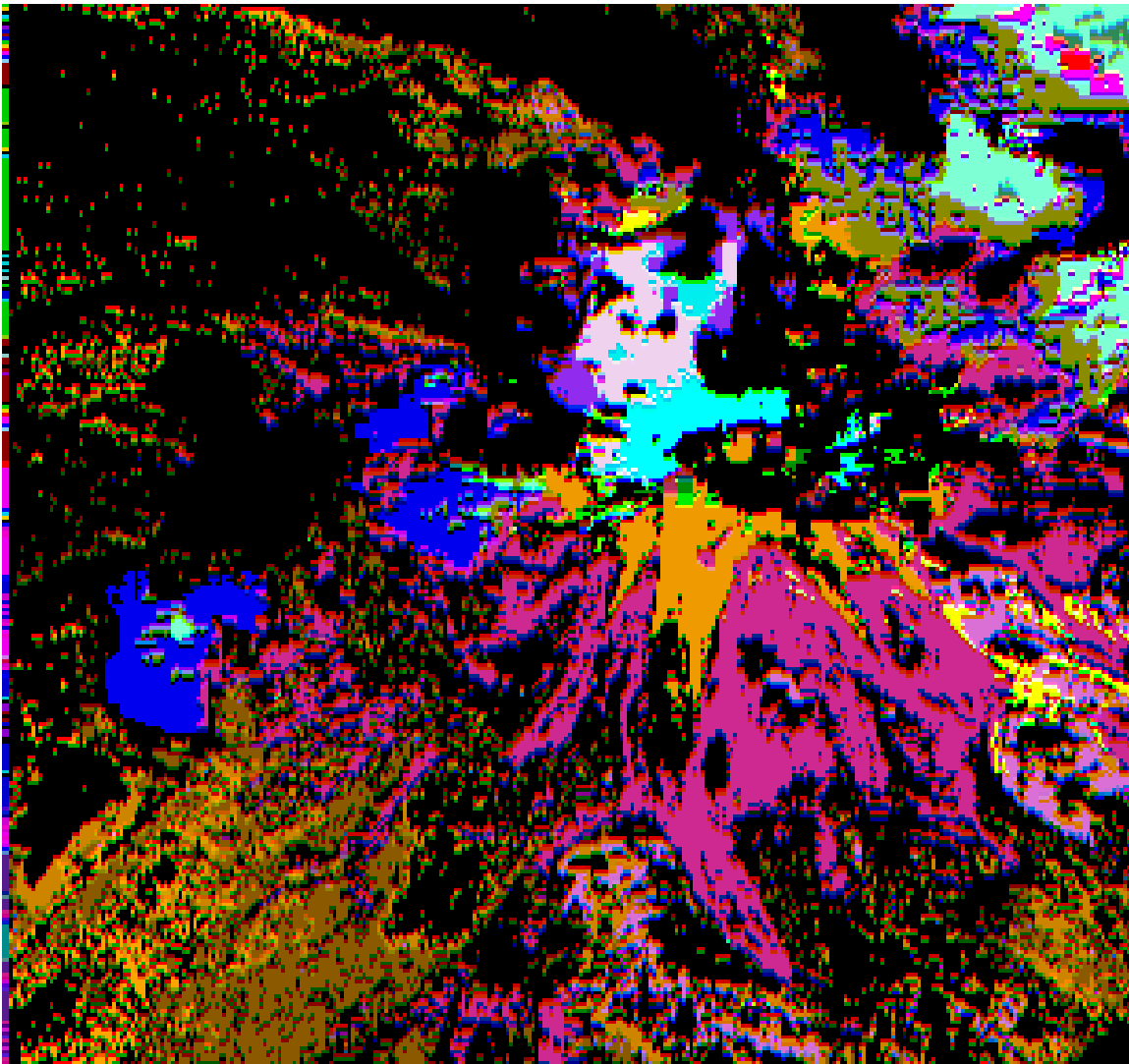


Figure 9. ENVI SAM classification using field sample reference spectra.

The SAM classification results were then compared to the USGS Spectral Library (see Figure 10) and some interesting results were produced: the mineral olivine was in high abundance due to the weathering of the mafic lavas; hydrothermal alteration minerals

Spectral Analyst			
File Options			
Unknown: PPI Curve			
Library Spectrum	Score	SAM	SFF
olivineg.spc	Olivine	[1.373]:	{0.501} {0.873}
andrad11.spc	Andradi	[1.339]:	{0.458} {0.882}
sanidin2.spc	Sanidin	[1.335]:	{0.420} {0.915}
andalusi.spc	Andalus	[1.335]:	{0.419} {0.916}
rutile2.spc	Rutile H	[1.335]:	{0.419} {0.916}
muscovi2.spc	Muscovi	[1.334]:	{0.418} {0.916}
actinol1.spc	Actinol	[1.334]:	{0.418} {0.916}
muscovi3.spc	Muscovi	[1.334]:	{0.418} {0.916}
muscovia.spc	Muscovi	[1.334]:	{0.418} {0.916}
topaz4.spc	Topaz Wig	[1.334]:	{0.418} {0.916}
muscovi1.spc	Muscovi	[1.334]:	{0.418} {0.916}
actinol2.spc	Actinol	[1.333]:	{0.419} {0.915}
talc2.spc	Talc HS21	[1.333]:	{0.418} {0.915}
hornble3.spc	Hornble	[1.333]:	{0.422} {0.911}
monazite.spc	Monazit	[1.333]:	{0.418} {0.915}
muscovib.spc	Muscovi	[1.333]:	{0.418} {0.915}
lepidol2.spc	Lepidol	[1.333]:	{0.417} {0.915}
holmquis.spc	Holmqui	[1.332]:	{0.421} {0.911}
actinol5.spc	Actinol	[1.331]:	{0.418} {0.913}
chrysoti.spc	Chrysot	[1.329]:	{0.418} {0.911}
cinnabar.spc	Cinnaba	[1.329]:	{0.418} {0.911}
muscovi7.spc	Muscovi	[1.328]:	{0.417} {0.911}
datolit2.spc	Datolit	[1.328]:	{0.417} {0.910}
carnall2.spc	Carnall	[1.327]:	{0.417} {0.910}
topazc.spc	Topaz Lit	[1.327]:	{0.417} {0.910}
actinol3.spc	Actinol	[1.327]:	{0.417} {0.910}
lepidol5.spc	Lepidol	[1.327]:	{0.417} {0.910}
rivadavi.spc	Rivadav	[1.326]:	{0.417} {0.909}
hornble1.spc	Hornble	[1.325]:	{0.417} {0.908}
galena6.spc	Galena S	[1.324]:	{0.421} {0.903}
muscovi5.spc	Muscovi	[1.322]:	{0.417} {0.905}
limonite.spc	Limonit	[1.321]:	{0.417} {0.904}
muscovic.spc	Muscovi	[1.321]:	{0.417} {0.904}
muscovi8.spc	Muscovi	[1.321]:	{0.417} {0.904}
almand4.spc	Almandin	[1.320]:	{0.417} {0.903}
hapatite.spc	Hydroxy	[1.320]:	{0.417} {0.903}
kainite.spc	Kainite	[1.320]:	{0.417} {0.903}
actinol4.spc	Actinol	[1.319]:	{0.417} {0.902}
almand2.spc	Almandin	[1.319]:	{0.417} {0.901}
goethit1.spc	Goethit	[1.318]:	{0.417} {0.901}
sphaler3.spc	Sphaler	[1.318]:	{0.417} {0.901}
riebeck1.spc	Riebeck	[1.318]:	{0.417} {0.900}
jarosit2.spc	Jarosit	[1.318]:	{0.417} {0.900}
mizzoni1.spc	Mizzoni	[1.317]:	{0.417} {0.900}
talc4.spc	Talc TL270	[1.316]:	{0.417} {0.899}
grossul3.spc	Grossul	[1.316]:	{0.417} {0.899}
spessar2.spc	Spessar	[1.316]:	{0.417} {0.899}

Figure 10. ENVI Spectral Analyst matching results.

such as goethite, hematite, and jarosite were suggested but not differentiated; and few clay minerals such as kaolinite were identified near the crater. These results may be accurate, but further refinement of the classification methods will be necessary to properly represent the mineralogy of the study area. Few morphological features were apparent from the classified image; however, additional imagery will be investigated to determine the major morphological features.

Conclusions

AVIRIS hyperspectral data and imagery are very useful for the mineralogical classification of volcanic features. Correction, processing, and analysis are laborious but powerful; the tools provided by ENVI are adequate, but extensive knowledge of the study area is required to avoid misrepresentation of the results. Further analysis and processing will be required to improve this introductory classification.

References

Carrasco-Nunez, G., 1996. "Lava flow growth inferred from morphometric parameters: a case study of Citlaltepctl volcano, Mexico."

Green, et al., 1998. "Imaging spectroscopy and the Airborne Visible/Infrared Imaging Spectrometer (AVIRIS)."

Zimelman, et al., 2003. "Stratovolcano stability assessment methods and results from Citlaltepctl, Mexico."

Jensen, J. R., 2005. "Introductory digital image processing: a remote sensing perspective."

"FLAASH User's Guide"—ENVI Online Help